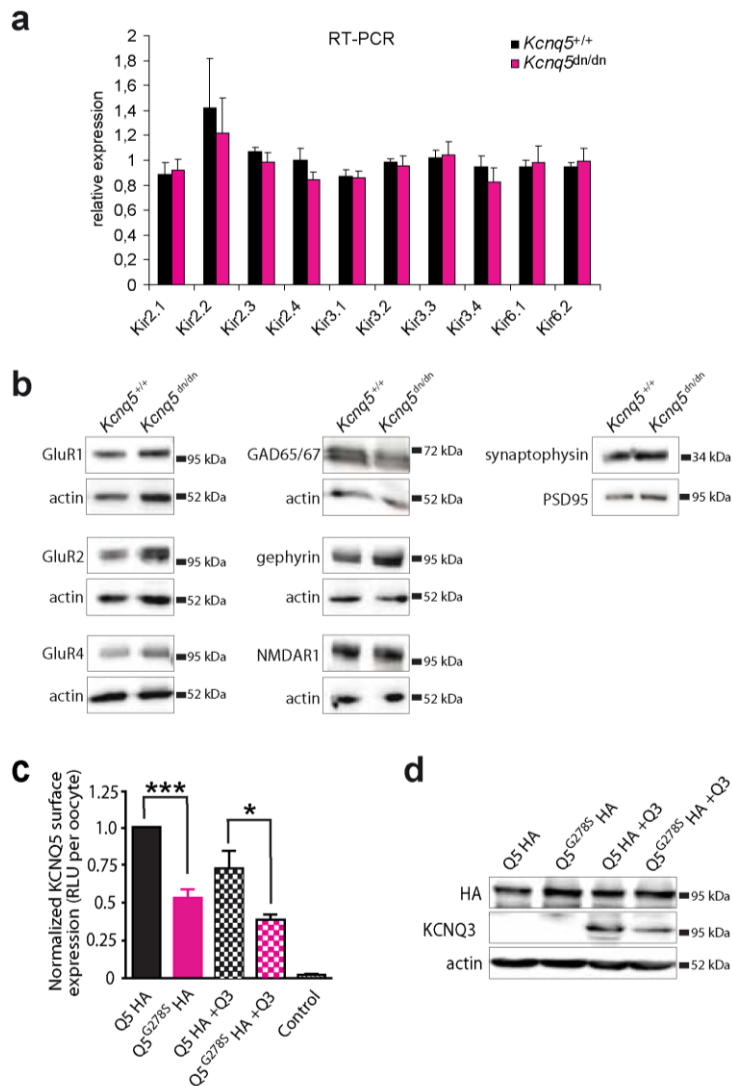
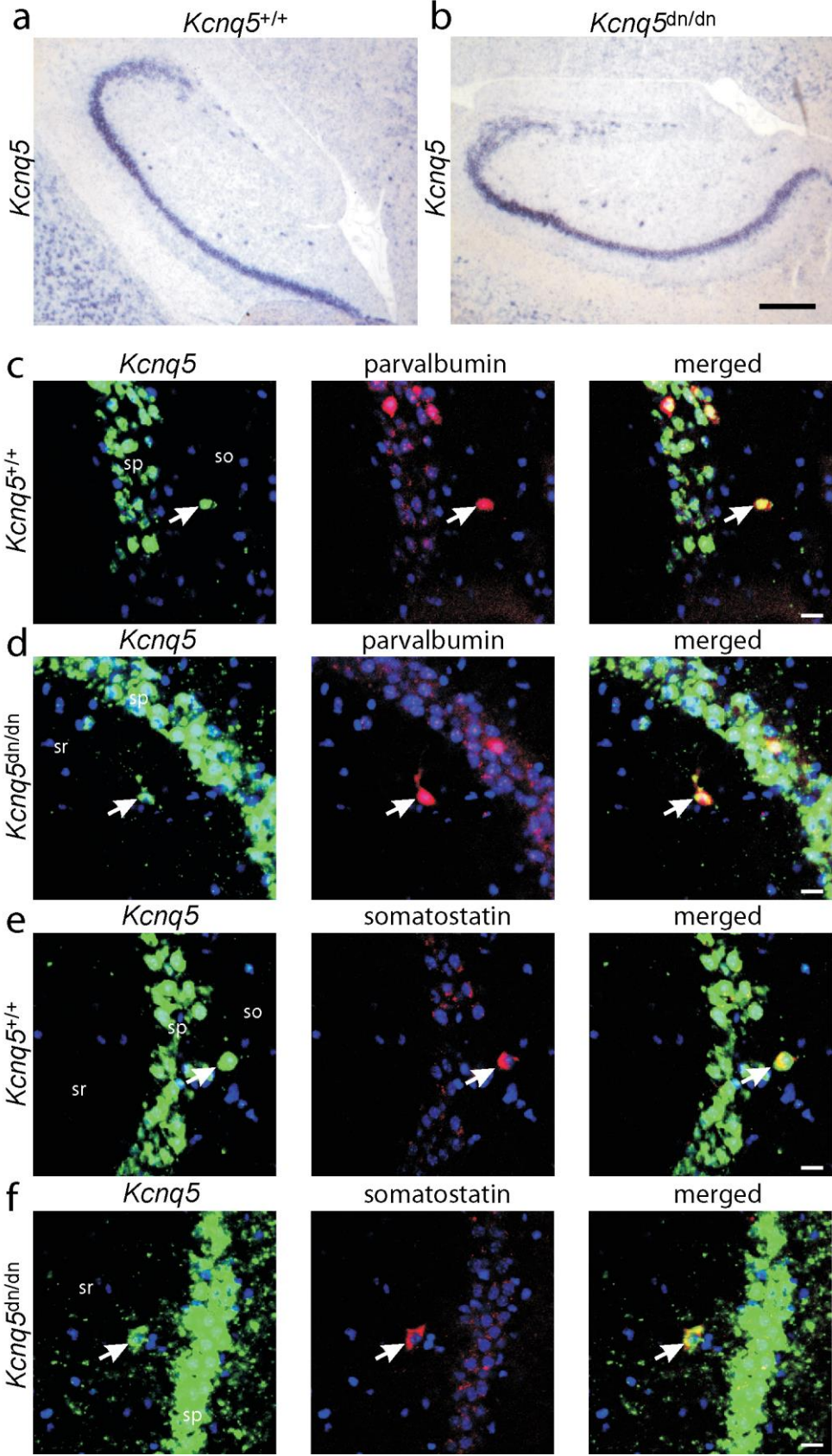


Supplementary Figure 1: Expression controls and surface residence of mutant KCNQ5



(a) Quantitative real-time PCR demonstrates that the expression of inwardly rectifying *Kir* K^+ channels is not changed in brains of *Kcnq5*^{dn/dn} mice. **(b)** Western blot analysis demonstrates unchanged expression levels of selected synaptic proteins between the genotypes. Whole brain membrane preparations from adult *Kcnq5*^{+/+} and *Kcnq5*^{dn/dn} mice were probed with antibodies against GluR1, GluR2, GluR4, GAD65/67, gephyrin, NMDAR1, synaptophysin and PSD95. Actin served as loading control. **(c)** Cell surface expression of epitope-tagged WT KCNQ5 (black) and dominant-negative KCNQ5^{G278S} (red) protein in *Xenopus* oocytes, either by itself (solid columns) or co-expressed with KCNQ3 at a 3:1 Q5:Q3 ratio (checked columns). Non-injected oocytes served as control (at least 6-8 oocyte batches per genotype with $n > 20$ oocytes per batch, $*p < 0.05$, $***p < 0.001$; Student's t-test). **(d)** Western blot analysis of KCNQ subunits ascertains comparable total protein levels in *Xenopus* oocytes used in **(c)**. Actin, loading control.

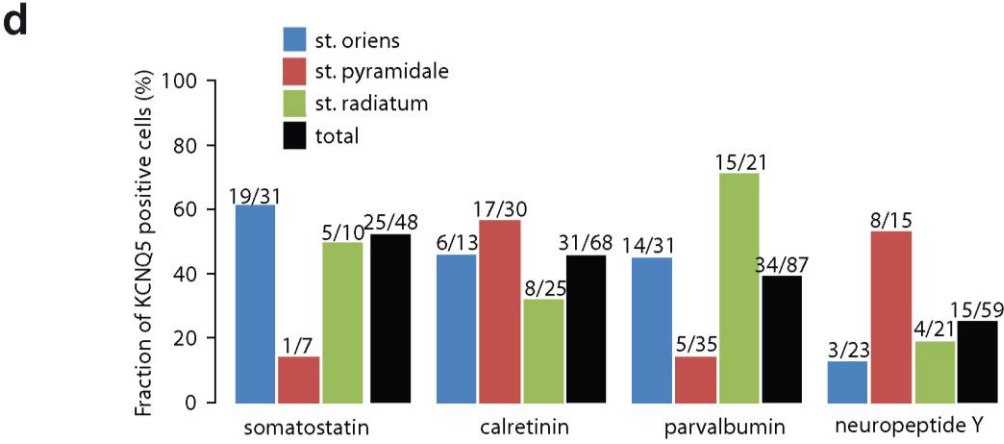
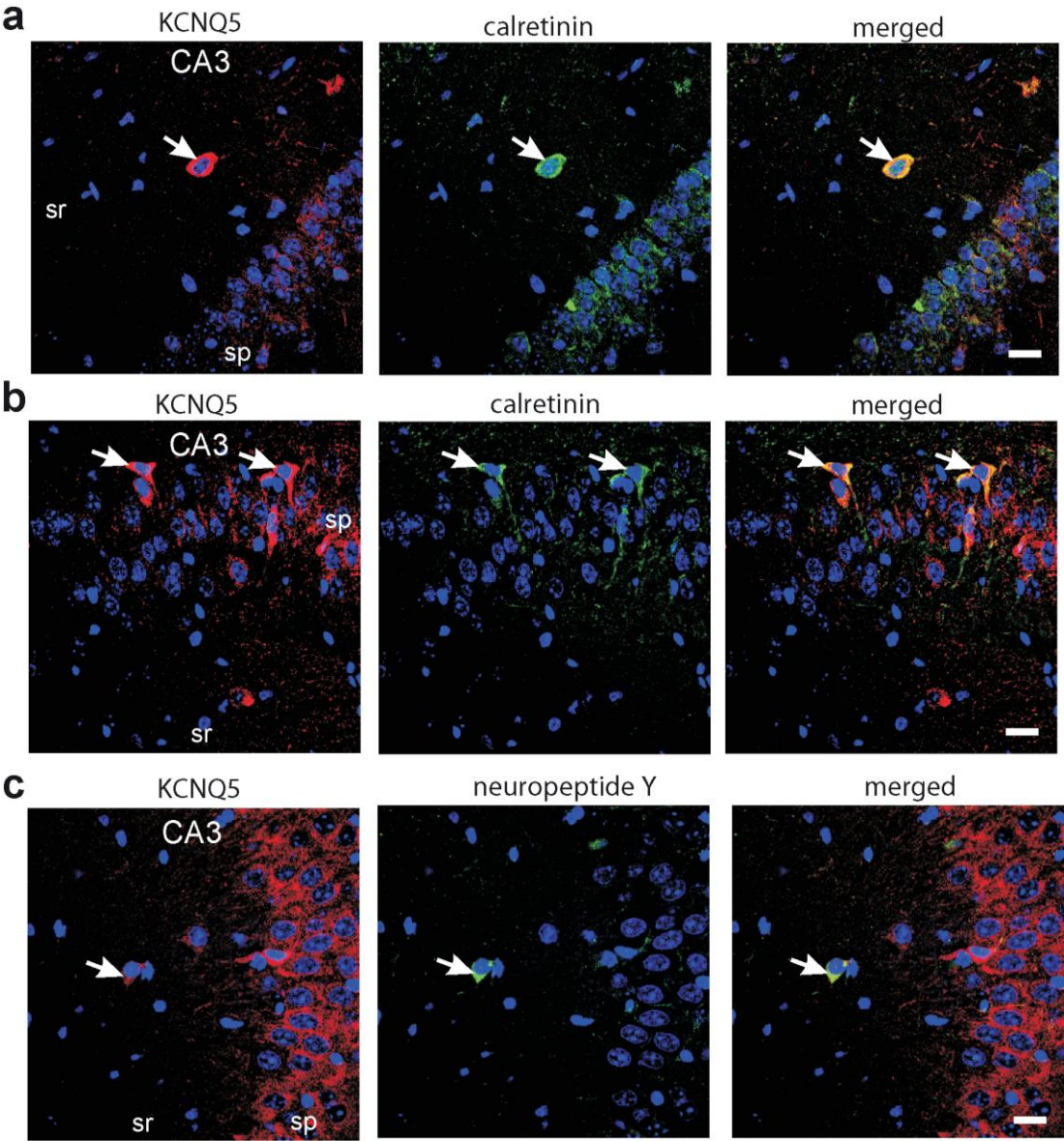
Supplementary Figure 2: Expression of *Kcnq5* mRNA in hippocampal interneurons



(a,b) *Kcnq5* expression in *Kcnq5*^{+/+} (a) and *Kcnq5*^{dn/dn} (b) hippocampi as revealed by *in situ* hybridization. (c-f) *Kcnq5* expression in CA3 interneurons. Hippocampi of *Kcnq5*^{+/+} (c) and

Kcnq5^{dn/dn} (**d**) mice were labeled with *Kcnq5 in-situ* probe (green) and parvalbumin antibody (red). Parvalbumin-positive interneurons co-labeled for *Kcnq5* are highlighted by arrows. *Kcnq5 in-situ* hybridization in *Kcnq5*^{+/+} (**e**) and *Kcnq5*^{dn/dn} (**f**) hippocampi followed by somatostatin antibody labeling shows expression of *Kcnq5* in somatostatin positive interneurons (arrows). Nuclei were labeled with DAPI (**c-f**,blue). Scale bar for (**a,b**): 250µm and 20µm for (**c-f**). sp: st. pyramidale; sr: st. radiatum; so: st. oriens.

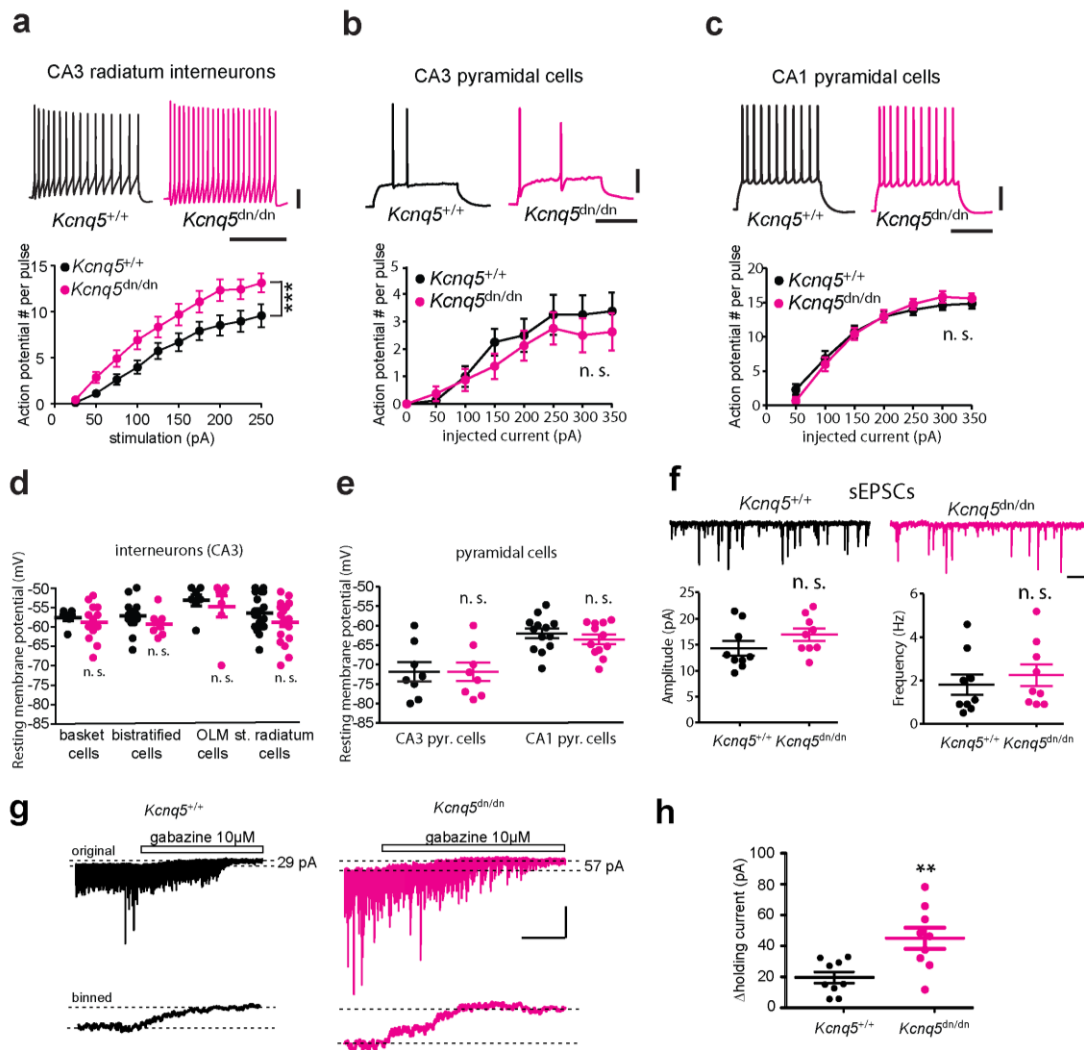
Supplementary Figure 3: KCNQ5 in interneurons of *Kcnq5^{dn/dn}* mice



(a,b) Co-labeling of calretinin-positive interneurons in st. radiatum (a) and st. pyramidale (b) of the CA3 region with KCNQ5 antibody. (c) Co-labeling of neuropeptide Y (NPY)-positive

interneuron in st. radiatum of the CA3 region with KCNQ5 antibody. Scale bars (**a-c**), 20 μm . (**d**) Proportion of interneurons unambiguously co-labeled for KCNQ5 and in interneuron subtype markers identified by labeling for parvalbumin, somatostatin, calretinin, and neuropeptide Y (NPY). Results are subgrouped according to the location of the cell body in the st. oriens, st. pyramidale, and st. radiatum, and as sum for all regions. The given percentage is likely to represent a lower limit since weakly KCNQ5-stained cells may have escaped our analysis.

Supplementary Figure 4: Electrical properties of neurons in hippocampal slices

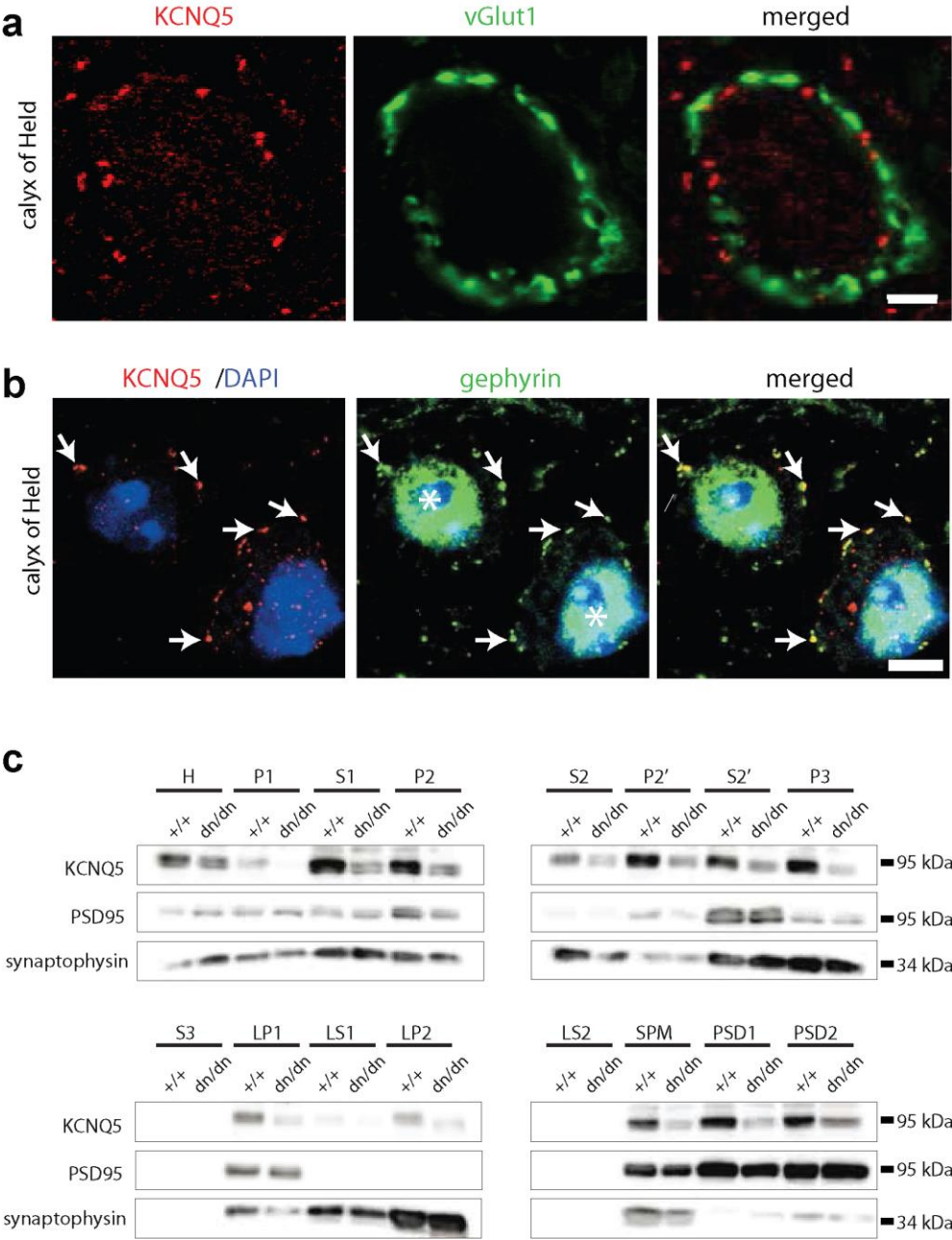


(a-c) Electrical excitability of hippocampal neurons as assessed by action potential firing during current injections. (a) *Kcnq5*^{dn/dn} CA3 st. radiatum interneurons (identified by GAD-promotor driven GFP fluorescence; average of diverse subtypes which were not classified by biocytin filling) show higher excitability than WT interneurons, similar to CA3 st. oriens and st. pyramidale interneurons (Fig. 2). (WT: 18 cells, 7 mice; *Kcnq5*^{dn/dn}: 19 cells, 7 mice); ***p < 0.001 (ANOVA). (b,c) Intrinsic excitability of pyramidal cells in the CA3 (b) (WT: 8 cells, 3 mice; *Kcnq5*^{dn/dn}: 8 cells, 3 mice, n.s.) and CA1 area (c) (WT: 13 cells, 4 mice; *Kcnq5*^{dn/dn}: 12 cells, 4 mice, n.s.) is not changed in *Kcnq5*^{dn/dn} mice. Top: Example traces recorded upon injection of 150 pA depolarizing current. Bottom: Number of action potentials (mean ± SEM) per 400 ms depolarizing pulse plotted against amplitude of injected current. Scale bars: 20 mV, 200 ms.

(d,e) Resting membrane potentials of hippocampal interneurons (d) and pyramidal cells (e) are not changed in *Kcnq5*^{dn/dn} mice. Resting potentials of individual cells (dots) and corresponding means ± SEM (lines) are shown. (f) Analysis of spontaneous EPSCs (WT and

Kcnq5^{dn/dn}: 9 cells, 3 mice, n.s.) with example traces (above) and mean values for amplitude and frequency for each recorded cell (below). Mean values and SEM are indicated by lines. Scale bars: 1 s, 20 pA. **(g,h)** Tonic inhibition is enhanced in *Kcnq5*^{dn/dn} mice as unveiled by difference in the change of holding current necessary to clamp CA3 pyramidal cells to -70 mV upon block of GABA_A receptors of (10μM gabazine). **(g)** Example traces of currents at -70 mV holding potential from WT and *Kcnq5*^{dn/dn} CA3 cells. Below original traces, binned traces are shown in which sIPSC have been removed to highlight the difference between WT and *Kcnq5*^{dn/dn} CA3 cells. Dashed lines below correspond to dashed lines in original traces. Scale bars: 200 pA (top traces), 50 pA (bottom traces), 40 s. **(h)** Values for holding current reduction for individual cells shown as dots and for mean and SEM values as lines (WT: 9 cells, 3 mice; *Kcnq5*^{dn/dn}: 9 cells, 3 mice) **p<0.01 (Student's t-test).

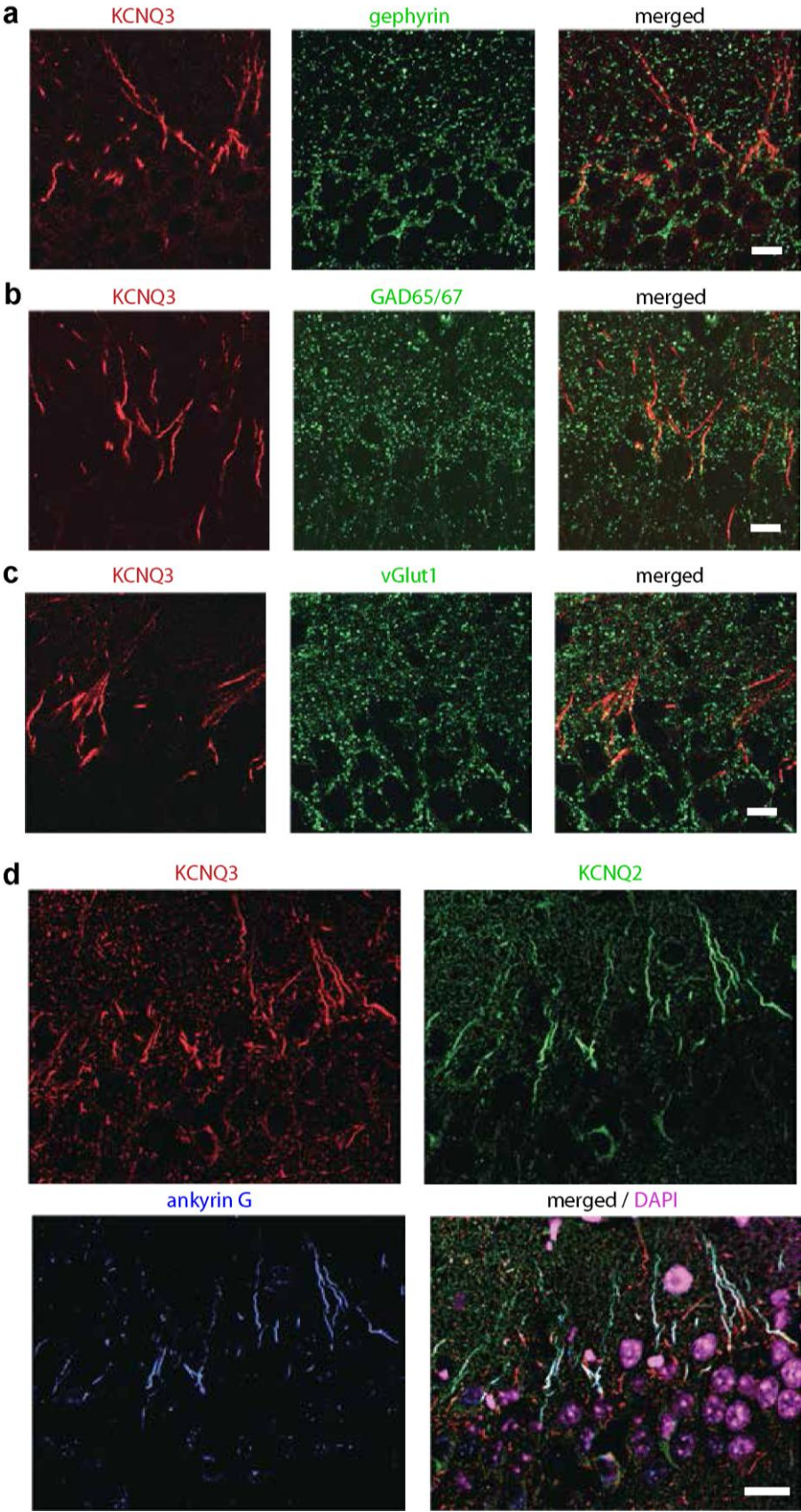
Supplementary Figure 5: Synaptic localization of KCNQ5



(a,b) Localization of KCNQ5 in murine calyx of Held. Calyx of Held labeled with KCNQ5 (red), vGlut1 (**a**, green) or gephyrin (**b**, green) antibodies. No co-localization of KCNQ5 and the excitatory synaptic protein vGlut1 (**a**). Co-localization of KCNQ5 and gephyrin (**b**, arrows), with nuclei stained by DAPI. Unspecific gephyrin labeling of nuclei (Essrich et al., Nat Neurosci 1: 563-571 (1998).) indicated by asterisk. Scale bars: 5 μ m. **(c)** Subcellular fractionation of total brain lysates of adult *Kcnq5*^{+/+} and *Kcnq5*^{dn/dn} mice. Subcellular compartments probed with antibodies against KCNQ5, PSD95 and synaptophysin. KCNQ5 and PSD95 proteins are enriched in the postsynaptic density fractions (PSD1 and PSD2). Note reduced KCNQ5 protein levels in *Kcnq5*^{dn/dn} compared to *Kcnq5*^{+/+} mice, which is more

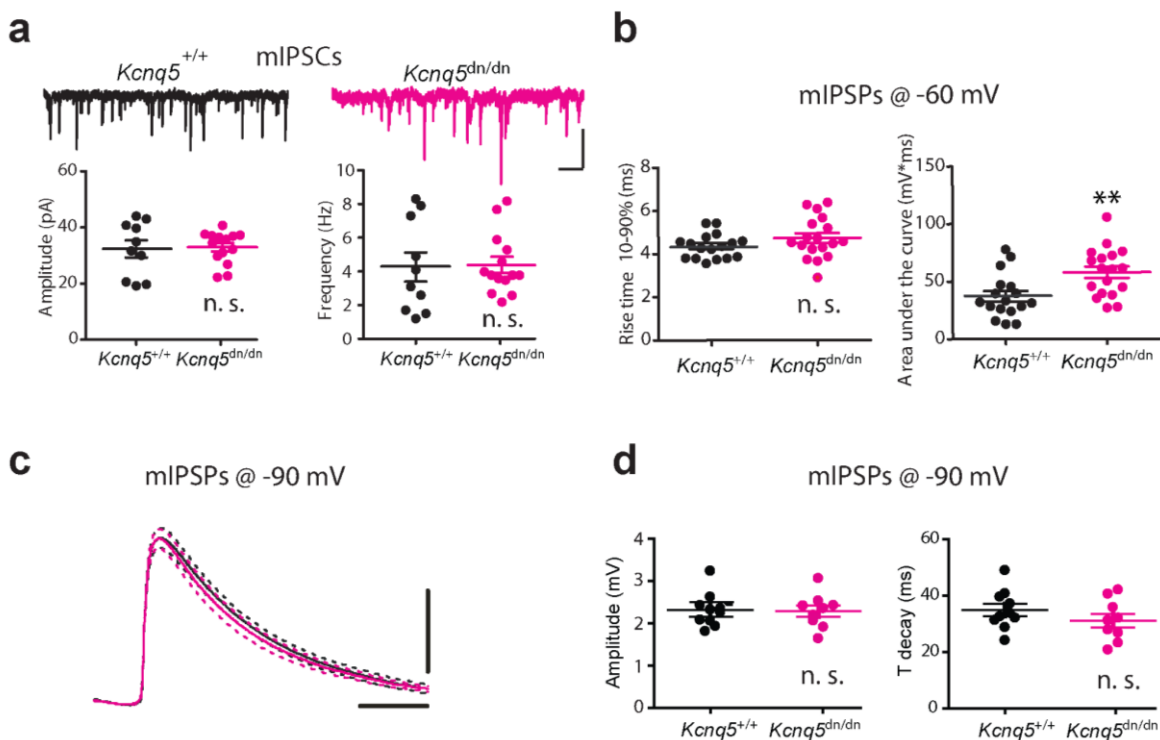
pronounced in synaptic fractions than in total homogenate. H: total homogenate; P1: nuclei and large debris; P2 and P2': crude synaptosomal membrane fractions; P3: light membrane fraction; LP1: synaptosomal membrane fraction; LP2: synaptic vesicle-enriched fraction; SPM: synaptic plasma membranes; PSD1+2: post-synaptic density fractions. S1, S2, S2', S3, LS1 and LS2 are supernatants from P1, P2, P2', P3, LP1 and LP2, respectively. Western blots representative for 3 experiments with 3 mice per genotype and experiment are shown.

Supplementary Figure 6: KCNQ2 and -3 at axon initial segments of pyramidal cells



(a-c) No co-localization of KCNQ3 (red) with the synaptic proteins gephyrin (a, green), GAD65/67 (b, green) or vGlut1 (c, green) in the CA1 region of mouse hippocampus. (d) Triple staining of murine CA1 pyramidal cells with KCNQ3 (red), KCNQ2 (green) and the axon initial segment protein ankyrin G (blue). Nuclei were labeled with DAPI (magenta). Scale bars: for (a-c): 10 μm , for (d): 20 μm .

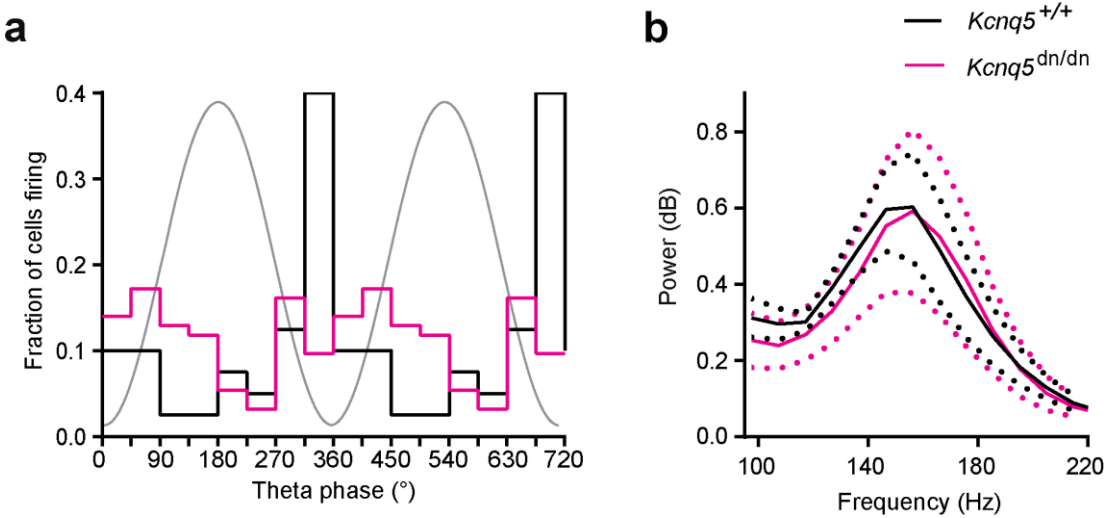
Supplementary Figure 7: Synaptic transmission onto CA3 neurons



(a) Summary of miniature IPSCs recordings in hippocampal slices (WT and $Kcnq5^{dn/dn}$: 10 cells, 4 mice each, n.s.) with example traces and mean values for amplitude and frequency for each recorded cell. Scale bars: 1 s, 50 pA. (b) Summary of mIPSP rise time and area under the curve. ** $p < 0.01$ (Student's t-test).

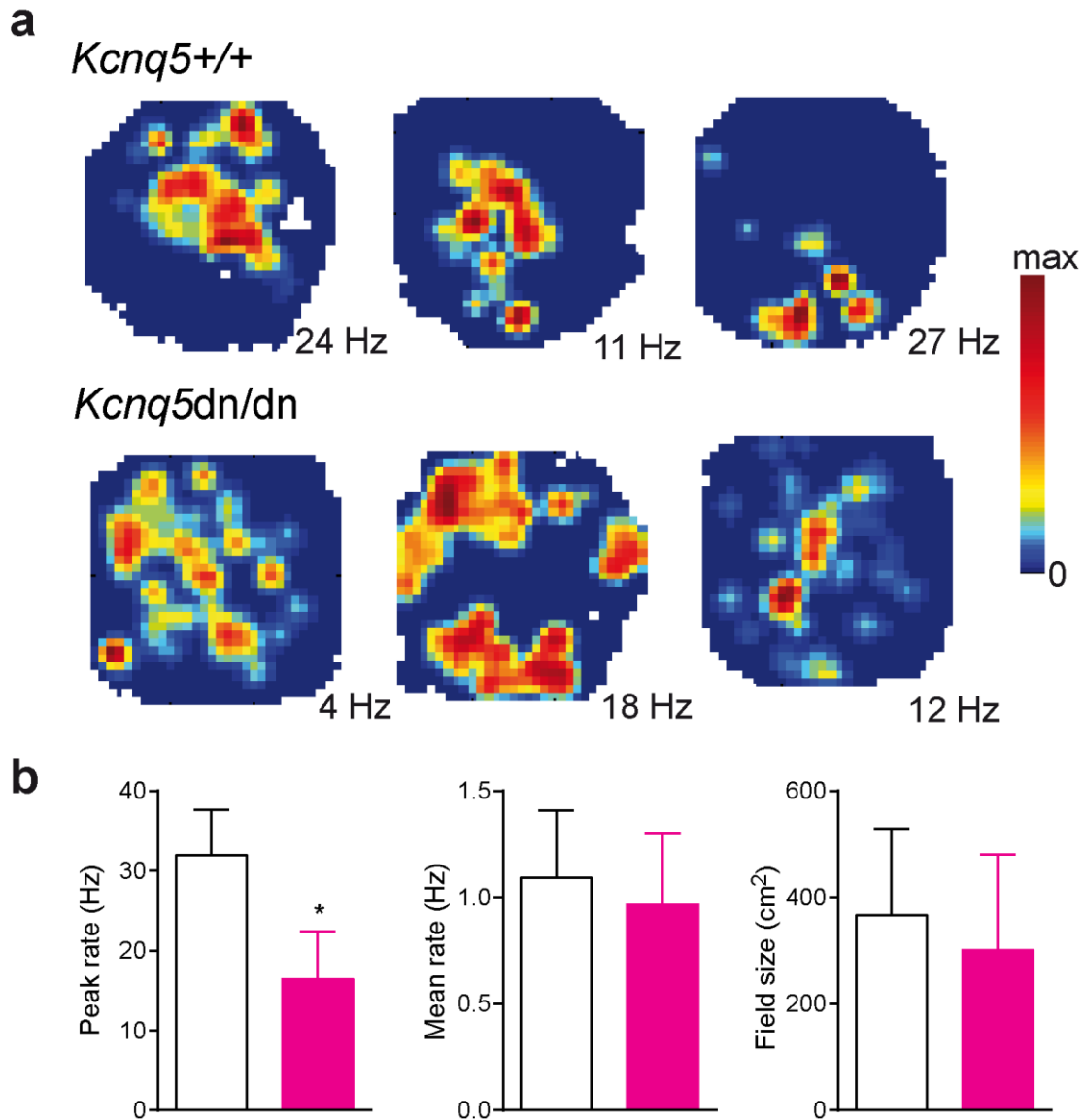
(c) Miniature inhibitory postsynaptic potentials (mIPSPs) recorded at -90 mV do not differ in amplitude or decay kinetics between WT (black, 10 cells, 3 mice) and $Kcnq5^{dn/dn}$ mice (red, 9 cells, 3 mice). Averaged time courses of mIPSPs (solid lines). Dotted lines show the corresponding 95% confidence interval. Scale bars: 1 mV, 20 ms. (d) Mean IPSP amplitudes and decay times for each recorded cell. Mean values averaged over all cells and corresponding SEM indicated by lines.

Supplementary Figure 8: Discharge of CA1 cells and network synchronization *in vivo*



(a) Theta phase preference of CA1 pyramidal cell firing (WT: 40 cells, 4 mice, *Kcnq5^{dn/dn}*: 93 cells, 5 mice, $p < 0.05$). Grey line - reference theta oscillation cycle. (b) Power spectral density of ripple oscillations in the CA1 area *in vivo* (mean \pm SEM; WT: 10 mice, *Kcnq5^{dn/dn}*: 11 mice).

Supplementary Figure 9: Properties of place cells in the CA3 area



(a) Representative firing maps of CA3 pyramidal cells recorded in a circular arena. The spiking activity at each particular location is color-coded (linear scale from zero to max shown on the left). Firing rate in each spatial bin is normalized to the peak firing rate of respective place cells which is given as number in the right lower corner of each map. (b) Spatial firing properties of CA3 pyramidal cells: peak rate (highest firing rate across all spatial bins), mean rate (over all spatial bins) and place field size (WT: 18 cells, 4 mice, *Kcnq5*^{dn/dn}: 11 cells, 4 mice, * $p < 0.05$, ANOVA, population means \pm SEM).

Supplementary Table 1: Local field potential oscillations

	<i>Kcnq5</i> ^{+/+}	<i>Kcnq5</i> ^{dn/dn}
CA1, cumulative theta (5-10 Hz) power, au	25.05±2.23	27.94±2.51
CA1, cumulative gamma (35-85 Hz) power, au	11.90±3.48	5.51±0.41 *
CA1, ripples: goodness of sin-fit	0.46±0.02	0.43±0.03
CA1, ripples: fast (160-200 Hz) to slow (100-120 Hz) power ratio	4.27±0.92	4.39±0.84
CA1, cumulative ripple power, mV ² *Hz ⁻¹	2.89±0.68	2.89±1.06
CA3, cumulative theta (5-10 Hz) power, au	14.32±0.94	13.13±1.55
CA3, cumulative gamma (35-85 Hz) power, au	4.86±0.63	2.90±0.56 *

au - arbitrary units, *p<0.05 (Student's t-test or Wilcoxon rank sum test preceded by Lilliefors test)

Supplementary Table 2: Properties of CA1 place cells

	<i>Kcnq5</i> ^{+/+} (n=37)	<i>Kcnq5</i> ^{dn/dn} (n=36)
Peak rate, Hz	18.31±1.58	18.81±1.94
Mean rate (MR), Hz	1.23±0.13	1.64±0.15 *
Field size, cm ²	544.68±93.58	1119±39.76 ****
MR in field, Hz	5.58±0.57	4.54±0.23
Spatial coherence	0.44±0.04	0.50±0.03

*p<0.05; ****p<0.0001 (Wilcoxon rank sum test)

Supplementary methods

Quantitative real-time PCR for *Kir* K⁺ channels

Total RNA was prepared from hippocampi of 6 WT and 6 *Kcnq5*^{dn/dn} mice using TRIZOL (Invitrogen), digested with RNase-free DNase and purified with RNeasy columns (Qiagen). cDNA synthesis used SuperScript II reverse transcriptase, random primer, first-strand reaction buffer, 0.1 M DTT, 10 mM dNTP mix, and RNaseOUT (Invitrogen). SYBR green PCR master mix (Applied Biosystems) was taken to run the quantitative RT-PCR assay. Triplicates were used for every animal and gene. Following primers were used: TCTCACTTGCTTCGGCTCATTCTC (*Kir2.1*), CCAGAGAACTTGTCCTGTTGCTG (*Kir2.1*), TCCTGGCCTAGACAGAAACAGC (*Kir2.2*), GGCACCTTCATGGGCTTGTTTAGC (*Kir2.2*), TGGTGTGGGTTTGGGTACAGAG (*Kir2.3*), TGGAACTGGAGGGACTGCAAG (*Kir2.3*), ACAGCTCTAGGAGGTAGACACTGC (*Kir2.4*), TGATCGTCCAGGCTCTTGCTTG (*Kir2.4*), TCCGCTGCAAGCTGCTCAAATC (*Kir3.1*), GATCACGTGGCAAATTGTGAGAGG (*Kir3.1*), AGGCGATCAGGATGGAGTGAAC (*Kir3.2*), AATCGCCTTCCAAGACGTTAGTC (*Kir3.2*), TCCACTGCATCCTTGTCTTGCC (*Kir3.3*), AGGTCCATTGCCATGCTGTTGC (*Kir3.3*), AGAAGCTCTCTGCGCTACAAGG (*Kir3.4*), TGGTGATCTGATGCTGCCATGC (*Kir3.4*), AAGGCACCATGGAGAAGAGTGG (*Kir6.1*), ACGCAGACGTGAATGACCTGAC (*Kir6.1*), ACTCTCAGAGCAGTGTGGTGTC (*Kir6.2*), TCACAGGTGGGAGGCTTTATGAC (*Kir6.2*). For quantification, we used the $2^{-\Delta\Delta Ct}$ method, taking beta-actin as reference gene.

Western Blotting

Protein samples were separated on reducing 8.5% sodium dodecyl sulfate-polyacrylamide gels. Proteins were blotted to polyvinylidene difluoride membranes (Roth) using a semidry blotting system (TE77, Hoefer). Blots were blocked for 30 min at RT (5% milk powder in Tris-buffered saline (TBS)) and probed with appropriate antibodies. Washing steps were performed with 0.1% (v/v) Tween 20 in TBS. Detection was performed via ECL Western blot substrate. Blots were imaged with a PeqLab camera system or X-ray film and Curix60 processor (AGFA).

The following antibodies were used for Western blots: rabbit anti-KCNQ5, 1:600, rat anti-HA 3F10 (Roche, 1:1,000); mouse anti-actin (Sigma, 1:2,000); mouse anti-PSD95 (Calbiochem, 1:2,000); mouse anti-synaptophysin (Synaptic Systems, 1:5,000); rabbit anti-GluR1 (Chemicon; 1:1,000); mouse anti-GluR2 (Abcam; 1:1,000); rabbit anti-GluR4 (Millipore; 1:1,000); mouse anti-GAD65/67 (Biotrend; 1:1,000); mouse anti-gephyrin (Synaptic Systems m7Ab; 1:500); mouse anti-NMDAR1 (Synaptic Systems; 1:1,000). Secondary antibodies were coupled to horseradish peroxidase (Chemicon, 1:10,000).

Determination of KCNQ5 surface expression

As described previously (Schwake et al., J. Biol. Chem. 275(18): 13343-13348 (2000)), a HA-tag was added to the extracellular loop of human KCNQ5 and KCNQ5^{G278S}, respectively. The resulting sequence between S1 and S2 transmembrane domains is ¹¹⁵PEHTKLASSN**SEHYPYDVPDYAVTFEERDKCPEWNCLLIL**¹²⁸ (HA epitope in bold type, residues derived from CIC-5 in italics). The surface expression of KCNQ proteins was determined as described (Schwake et al., J Biol Chem. 275: 13343-13348 (2000)). Water injected oocytes were used as negative control. Chemiluminescence signals (RLU) were normalized to KCNQ5-HA and compared using Student's unpaired two-tailed t-test. Oocytes were then pooled and homogenized in 1 M Tris, 1 M NaCl, 0.5 M EDTA, 1 mM Pefabloc® (Roche), 1x Complete® protease inhibitor mix (Roche) for Western blot analysis.

***In situ* hybridization**

In situ hybridization was carried out as previously described (Abe et al., Neurosci Res. 63:138-48 (2009)). Briefly, hippocampi were freshly embedded into OCT compound, cut into 16µm sections and stored at -80°C until use. Frozen sections were acetylated and incubated with 0.4ng/µl DIG-labeled KCNQ5 probe at 62°C over night in a hybridization buffer. The KCNQ5 probe for *in situ* hybridization was synthesized from cDNA with the following primers: ACGTCAGATAAGAAGAGCCGAG (forward) and GCAGGTGGTGACATCAGAAATA (reverse). The PCR product was cloned into pGEMTeasy vector (Promega), linearized and *in vitro* transcription was performed using DIG RNA labeling mix and Sp6 and T7 RNA Polymerase (Roche Diagnostics).

Sections were treated with RNaseA (Sigma-Aldrich) for 15 min at 37°C. To detect the hybridized probe, sections were incubated in 1% blocking reagent with alkaline phosphatase (AP)-conjugated sheep anti-DIG antibody (Roche Diagnostics) over night. AP activity was visualized with Nitro blue tetrazolium chloride/5-bromo-4-chloro-3-indolyl phosphate toluidine salt solution (NBT/BCIP, Roche Diagnostics). For immunostaining combined with *in situ* hybridization, hybridized sections were incubated for overnight with anti-Digoxigenin (Mouse) HRP conjugate (Perkin Elmer) and parvalbumin or somatostatin antibody. The RNA probe signal was detected with the TSA plus biotin system (Perkin Elmer) and Streptavidin, AlexaFluor 488 conjugate (Life technologies).

Subcellular fractionation

Dissected brains were homogenized (0.32 M sucrose, 4 mM HEPES, 1 mM Pefabloc® (Roche), 1x Complete® protease inhibitor mix (Roche)) using a Potter-Elvehjem with 9 strokes at 900 rpm. All steps were performed as described by Hallett et al. (Hallett et al., Curr. Protoc. Neurosci. 42: 1.16.1-1.16.16 (2008)) with following modifications: Homogenate

(H) centrifugation (1,000 x g, 10 min), supernatant (S1) centrifugation (12,000 x g, 10 min). Supernatant (S2) was centrifuged (260,000 x g, 2 h) to remain pellet (P3) and supernatant (S3). Pellet (P2) was resuspended in homogenization buffer (HB) and centrifuged (13,000 x g, 10 min). Resulting pellet (P2') was resuspended in 1.5 ml HB. 13.5 ml of ddH₂O were added for osmotic shock to release synaptic vesicles followed by homogenization with 3 strokes at 1,500 rpm. 95 µl 1 M HEPES (pH 7.4) were added and samples were rotated for 30 min and centrifuged (33,000 x g, 20 min) to collect pellet (LP1) containing synaptosomal membranes and the supernatant (LS1). LS1 was centrifuged (165,000 x g, 2 h) to receive pellet (LP2) containing synaptic vesicles. LP1 pellet was suspended in HB and added to a discontinuous gradient containing 0.8 to 1.0 to 1.2 M sucrose in HEPES and centrifuged (150,000 x g, 2 h). The interphase between 1.0 M and 1.2 M sucrose was recovered, diluted to 0.32 M sucrose and centrifuged (150,000 x g, 30 min). Pellet (SPM) containing synaptic plasma membranes was resuspended in SPM buffer (2 mM EDTA, 50 mM HEPES, 1 mM Pefabloc[®] (Roche), 1x Complete[®] protease inhibitor mix (Roche), pH 7.4). Triton X-100 was added to a final concentration of 0.5%. SPM was centrifuged (32,000 x g, 20 min) and pellet containing postsynaptic compartments was resuspended in SPM buffer (PSD1). Triton X-100 was added to a final concentration of 0.5% to ½ volume of PSD1. After rotation for 15 min and centrifugation (200,000 x g, 20 min), pellet (PSD2) was resuspended. 50 µg of each fraction were used for Western blot analysis. Due to lower protein concentration in PSD1 and PSD2 the maximum volume (equivalent to ~ 20-30 µg protein) was used. Experiments were repeated in 3 independent experiments (9 mice/genotype).